







Suprathermal Spontaneous Emissions in κ -distributed Plasmas

M. Lazar^{1,2} , S. Kim³, R. A. López², P. H. Yoon^{2,4,5,6} , R. Schlickeiser^{1,7} , and S. Poedts² 

¹ Institut für Theoretische Physik, Lehrstuhl IV: Weltraum- und Astrophysik, Ruhr-Universität Bochum, D-44780 Bochum, Germany; mlazar@tp4.rub.de

² Centre for Mathematical Plasma Astrophysics, Celestijnenlaan 200B, B-3001 Leuven, Belgium

³ Department of Physics, UNIST, Ulsan 44919, Republic of Korea

⁴ Institute for Physical Science and Technology, University of Maryland, College Park, MD, USA

⁵ School of Space Research, Kyung Hee University, Republic of Korea

⁶ Korea Astronomy and Space Science Institute, Daejeon 34055, Republic of Korea

⁷ Research Department of Complex Plasmas, Ruhr-Universität Bochum, D-44780 Bochum, Germany

Received 2018 September 21; revised 2018 November 8; accepted 2018 November 9; published 2018 November 21

Abstract

A suprathermal spectral component is identified in the spontaneous emissions of κ -distributed plasma populations, ubiquitous in astrophysical setups. Theoretical power spectra are confirmed by the simulations and capture the dispersion characteristics of electrostatic and electromagnetic eigenmodes of a quasi-stable magnetized plasma. Selectively enhanced by the suprathermal emissions are the fluctuations of fast modes (e.g., Langmuir, fast magnetosonic, or the low-wavenumber branches of kinetic Alfvén and Bernstein waves) induced resonantly by the energetic (suprathermal) particles. These results have an immediate implication in spectroscopic techniques of in situ or remote diagnosis for the very hot and dense plasmas, e.g., close to the Sun, where direct measurements of plasma particles and their properties are technically impossible. Contrasting patterns of suprathermal emissions may confirm the coronal origin of the suprathermal populations observed in the solar wind.

Key words: methods: analytical – methods: numerical – radiation mechanisms: non-thermal – radiation mechanisms: thermal – solar wind – Sun: corona

1. Introduction

Quasi-thermal motions of plasma particles trigger multiple physical processes via spontaneous emission and reabsorption (or induced emission) of random electromagnetic field fluctuations. Spontaneous fluctuations are detected in the quasi-stationary solar wind far from the influence of induced emissions, e.g., temperature anisotropies instabilities (Bale et al. 2009; Adrian et al. 2016), and are fully determined by the velocity distributions of plasma particles, making it possible to unveil their properties (Meyer-Vernet 1979; Meyer-Vernet & Perche 1989; Hoang et al. 1993; Maksimovic et al. 1995; Issautier et al. 1998; Moncuquet et al. 2005). Specifically, the quasi-thermal noise (QTN) spectroscopy enables us to determine macroscopic parameters such as plasma density and temperature profiles from in situ measurements of electrostatic noise (Meyer-Vernet & Perche 1989; Chateau & Meyer-Vernet 1991; Hoang et al. 1993; Maksimovic et al. 1995; Issautier et al. 1998; Zouganelis 2008; Moncuquet et al. 2005; Le Chat et al. 2009). Whatever the nature of the measured emissions, electrostatic or electromagnetic, spontaneous or induced, an accurate estimation of these emissions is essential for a reliable diagnosis. Advanced theories have thus been proposed to provide general formulations in unmagnetized (Schlickeiser & Yoon 2012) and multispecies magnetized plasmas (Navarro et al. 2014a), in order to show the influence of nonthermal populations on the dispersion and stability properties at ion and electron scales (Viñas et al. 2005, 2014, 2015; Navarro et al. 2015), and estimate the full wave-vector spectrum of spontaneous emissions in magnetized plasmas with nonthermal distributions (Kim et al. 2017, 2018; López & Yoon 2017; Yoon & López 2017). Spectroscopic techniques with improved theoretical estimates are of great interest for the new inner-heliospheric missions, such as the Parker Solar Probe (PSP) and the Solar Orbiter (SO;

Zouganelis 2008; Martinovic et al. 2018). Their scientific purpose is to investigate an outstanding problem of mutually related coronal heating and solar wind acceleration (Goldstein et al. 2015). The PSP mission, in particular, will reach an unprecedented low distance of $\sim 9.5R_S$ from the surface of the Sun (where $R_S = 6.957 \times 10^5$ km is the solar radius), where direct measurements of charged particles traveling along the almost radial interplanetary magnetic field lines will be prohibited owing to the heat shield that protects the spacecraft from intense solar heat and radiation. However, indirect measurement of QTN spectrum may be employed in order to diagnose the particle content. Spectral calibration originally developed for the solar wind near 1 au ($\approx 214R_S$) must be adjusted in order to reflect the fact that plasma in the outer corona is significantly magnetized. At 1 au the solar wind is low magnetized, or practically unmagnetized if we refer to electrostatic emissions in the range of electron plasma frequency $\omega_{pe} \simeq 24$ kHz; this is much higher than the electron cyclotron frequency, which is only $\Omega_e \simeq 0.16$ kHz (the ratio of the two frequencies being of the order $\mathcal{O}(10^2)$ or higher). However, at $\sim 9.5R_S$, $\omega_{pe} \simeq 570$ kHz, while $\Omega_e \simeq 59$ kHz, their ratio being on the order of 10 or less. For this parameter range, and in general for lower frequency emissions, which can be more informative in an alternative diagnosis (Viñas et al. 2005), the theory of fluctuations in magnetized plasmas must be employed. Another aspect that requires generalization involves the often-invoked electrostatic (ES) approximation (Meyer-Vernet et al. 2017), which may be an adequate first-order approximation, as recently pointed out Yoon et al. (2018), but for magnetized plasmas the QTN may contain significant magnetic field component that can be detected by the above-mentioned spacecraft. Specifically, the nearly identical Radio and Plasma Waves instrument on board SO and the *FIELDS* instrument suite for PSP (Müller et al. 2013; Bale et al. 2016) are capable of measuring magnetic field

fluctuations in the QTN range corresponding to 10^4 – 10^6 Hz, as long as the fluctuation intensity is above the instrument noise level of $\sim 10^{-11}$ [nT] 2 Hz $^{-1}$. This range of frequency coincides with the electric field measurements in the same range above the instrument noise level of 10^{-18} V 2 m 2 Hz $^{-1}$. With such unprecedented capabilities, these instruments may be able to detect a three-component magnetic field in the solar corona, from DC to beyond the electron cyclotron frequency to fully characterize magnetic field fluctuations. This in turn prompts the interest to decode and quantify the spontaneous emissions and upgrade the QTN spectroscopy to incorporate the effects of ambient magnetic field and the full electromagnetic spectrum.

2. Suprathermal Fluctuations

The solar wind is populated by suprathermal particles, which enhance the high-energy tails of their distributions (Vasyliunas 1968; Pierrard & Lazar 2010). Only a proper modeling incorporating these populations may clarify their implications, and in particular, the contribution to QTN, here called the *suprathermal* spontaneous emission. Idealized spectra of Maxwellian plasmas (Meyer-Vernet & Perche 1989; Hoang et al. 1993; Maksimovic et al. 1995; Moncuquet et al. 2005) have a limited relevance and may lead to inconsistent measurements, e.g., for the temperature, which depends on the measured energy range (Meyer-Vernet & Issautier 1998). The accuracy is improved by adopting a κ -distribution function (Chateau & Meyer-Vernet 1991; Zouganelis 2008; Le Chat et al. 2009; Martinovic et al. 2018) $F(v) = A_\kappa [1 + v^2/(\kappa w^2)]^{-\kappa-1}$, introduced 50 years ago Vasyliunas (1968) to reproduce the observed distributions with suprathermal tails (Pierrard & Lazar 2010). Here $A_\kappa = \Gamma(\kappa + 1)/\Gamma(\kappa - 1/2)/(\pi^{3/2} w^3 \kappa^{3/2})$ such that $\int dv F(v) = 1$, $\Gamma(z)$ is the gamma function, and the most-probable speed w is given by the second-order moment, which defines (for $\kappa > 3/2$) the isotropic scalar pressure and leads through the ideal gas law, $p = nk_B T$, to kinetic temperature (Meyer-Vernet et al. 2017). Quasi-thermal population is concentrated in the low-energy core, but suprathermal tails can markedly deviate from the (nearly) Maxwellian core (MC). Suprathermal fluctuations can therefore be outlined from a direct contrast with MC using recent estimations for the full spectrum of spontaneous emissions in magnetized plasmas (Kim et al. 2017, 2018; López & Yoon 2017; López et al. 2017; Yoon & López 2017).

However, contrasting κ - and Maxwellian models is, in general, subject to temperature invariance, invoking an equivalent Maxwellian (EM) $F_{EM}(v) = A \exp[-mv^2/(2k_B T)]$ of same temperature $T_{EM} = T = mv^2/(2k_B)$ (with $A = [m/(2\pi k_B T)]^{3/2}$), that enables to extend the concept of temperature of a κ -distribution in classical thermodynamics, but does not reproduce the core, see Figure 1, and, implicitly, it cannot be invoked to outline the suprathermal populations in a κ -distribution. Instead, the Maxwellian approaching the core (subscript MC; Vasyliunas 1968; Lazar et al. 2015), $F_{MC}(v) = \lim_{\kappa \rightarrow \infty} F(v) = A_M \exp[-v^2/w^2]$, with $A_M = 1/(\pi^{3/2} w^3)$, is defined by the same most-probable speed w but lower temperature $T_{MC} = mw^2/(2k_B) < T$, see Figure 1. Direct contrast of κ -distribution with this Maxwellian limit enables a straightforward evaluation of the suprathermal emissions. In terms of the electric field spectral intensity $\langle \delta E^2 \rangle_{\mathbf{k}, \omega} = \langle \delta E_{\mathbf{k}, \omega}^i \delta E_{\mathbf{k}, \omega}^{i*} \rangle$, as a function of wave-vector \mathbf{k} and wave-frequency ω , we compare the fluctuations for a κ -distribution $\langle \delta E^2 \rangle_{\mathbf{k}, \omega}^\kappa = \langle \delta E^2 \rangle_{\mathbf{k}, \omega}^{\text{total}}$ with thermal excitations of

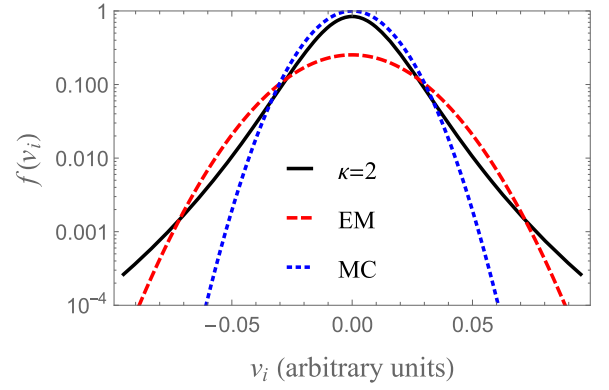


Figure 1. Contrasting κ -distribution (black, $\kappa = 2$) with EM (red-dashed) of same temperature, and Maxwellian limit approaching the core (MC, blue-dotted).

its core $\langle \delta E^2 \rangle_{\mathbf{k}, \omega}^\kappa = \langle \delta E^2 \rangle_{\mathbf{k}, \omega}^{\text{therm}}$, to find the suprathermal emissions

$$\langle \delta E^2 \rangle_{\mathbf{k}, \omega}^{\text{st}} = \langle \delta E^2 \rangle_{\mathbf{k}, \omega}^{\text{total}} - \langle \delta E^2 \rangle_{\mathbf{k}, \omega}^{\text{therm}}. \quad (1)$$

Intensities are computed (Kim et al. 2017, 2018) within cylindrical symmetry for distributions and fields (i.e., $\mathbf{k} = k_\perp \hat{\mathbf{e}}_1 + k_\parallel \hat{\mathbf{e}}_3$, where \perp and \parallel denote directions with respect to the uniform magnetic field)

$$\langle \delta E^2 \rangle_{\mathbf{k}, \omega} = \Lambda_{ij}^{-1}(\mathbf{k}, \omega) \Lambda_{ik}^{-1*}(\mathbf{k}, \omega) \sum_a \frac{2e_a^2 n_a}{\pi \omega^2} \sum_{n=-\infty}^{\infty} \int dv V_j^n V_k^{n*} \delta(\omega - k_\parallel v_\parallel - n\Omega_a) F_a(v), \quad (2)$$

with the linear dielectric tensor

$$\begin{aligned} \Lambda_{ij}(\mathbf{k}, \omega) &= \delta_{ij} - \frac{c^2 k^2}{\omega^2} \left(\delta_{ij} - \frac{k_i k_j}{k^2} \right) \\ &+ \sum_a \frac{\omega_{pa}^2}{\omega^2} \int dv \sum_{n=-\infty}^{\infty} \frac{V_i^n V_j^{n*}}{\omega - k_\parallel v_\parallel - n\Omega_a} \\ &\times \left(\frac{\omega - k_\parallel v_\parallel}{v_\perp} \frac{\partial F_a}{\partial v_\perp} + k_\parallel \frac{\partial F_a}{\partial v_\parallel} \right) \\ &+ \hat{\mathbf{e}}_i \hat{\mathbf{e}}_j \sum_a \frac{\omega_{pa}^2}{\omega^2} \int dv v_\parallel \left(\frac{\partial F_a}{\partial v_\parallel} - \frac{v_\parallel}{v_\perp} \frac{\partial F_a}{\partial v_\perp} \right). \quad (3) \end{aligned}$$

Subscript a denotes species of a plasma of electrons ($a = e$) and protons ($a = p$), $e_a = \pm e$ is the unit electric charge, n_a is the number density (satisfying charge neutrality $n_p = n_e = n_0$), $\Omega_a = e_a B_0 / (m_a c)$ is the cyclotron frequency (B_0 , m_a , and c are the ambient magnetic field, particle mass, and the speed of light, respectively), $\mathbf{V}^n = v_\perp (n J_n(b)/b) \hat{\mathbf{e}}_1 - i v_\perp J_n'(b) \hat{\mathbf{e}}_2 + v_\parallel J_n(b) \hat{\mathbf{e}}_3$, and $J_n(b)$ is the Bessel function (prime denotes the derivative) of the first kind of order n and argument $b = k_\perp v_\perp / \Omega_a$.

3. Theory versus Simulations

In a recent study of electromagnetic fluctuations, Viñas et al. (2005) originally suggested that a comparison of these emissions due to thermal and nonthermal distributions may provide a diagnostic signature by which inferences about the

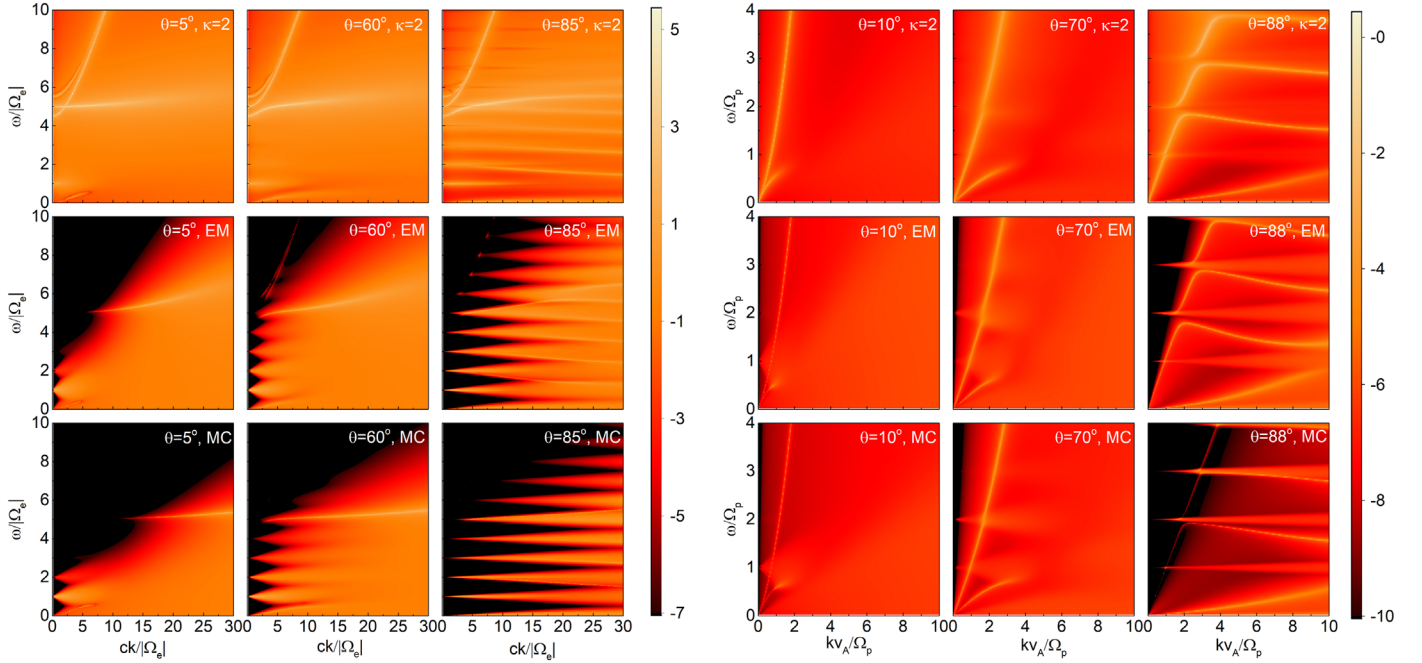


Figure 2. Fluctuations from theory: high frequency (left) and low frequency (right).

nature of the particle velocity distribution function can be ascertained without in situ particle measurements. Here, we look to the full spectrum of spontaneous fluctuations and first compare the estimates for a κ -distributed plasma with thermal emissions as given by EM and MC. Figure 2 displays frequency-wavenumber ($\omega - k$) spectra of spontaneous emissions predicted by the theory for three directions of propagation with respect to the magnetic field. The color bars show normalized versions of Equation (2) in logarithmic scale, i.e., $\log[2\pi^3|\Omega_e|\langle E^2 \rangle/T]$ for the high-frequency emissions (left panels) and $\log[2\pi^3|\Omega_p|\langle E^2 \rangle/T]$ for the low-frequency emissions (right panels). Responsible for the high-frequency emissions (left panels) are mainly the electrons, for which we set a coronal parametrization with $\omega_{pe} \equiv \sqrt{4\pi n_e e^2/m_e} = 5|\Omega_e|$, and either $v_{Te}/c = 0.1$ for κ -distribution with $\kappa = 2$ (top) and the EM (middle), or $v_{Te}/c = 0.05$ for MC (bottom). The low-frequency fluctuations (right panels) are obtained for $m_p/m_e = 1836$, $\kappa_e = \kappa_p = \kappa = 2$, Alfvén speed $v_A/c = 0.001$, and for the plasma beta parameters, either $\beta_p = \beta_e = 0.1$ for EM and κ -distributions or $\beta_p = \beta_e = 2.5 \times 10^{-2}$ for MC. The quasi-thermal energy of plasma particles transfers mainly to the collective (eigenmode) excitations, whose spectrum (markedly enriched in magnetized plasmas) is outlined by intensity peaks: the high-frequency Langmuir and R,L-modes (left panels), and the low-frequency magnetosonic/whistler and Alfvén (or ion-cyclotron (IC)) modes (right panels) in quasi-parallel directions ($k_{\parallel} \gg k_{\perp}$), while for highly oblique angles ($k_{\parallel} \ll k_{\perp}$) one can distinguish the ordinary (O) and extraordinary (X) modes, or the kinetic Alfvén and multiple harmonic cyclotron (Bernstein) waves. Quantified by the low values of κ , the abundance of suprathermals, and, implicitly, their effects, are outlined by contrasting κ -distribution with MC. Thermal fluctuations obtained for MC are at the lowest level, lower than thermal emissions of EM, and much lower than quasi-thermal (total) emissions of κ -distribution.

This simulation of spontaneous fluctuations by the suprathermals is confirmed by the simulations, see Figure 3 with color bars showing $\log[\langle E^2 \rangle/B_0^2]$. High-frequency fluctuations (left panels) are obtained from particle-in-cell simulations with a realistic mass ratio $m_p/m_e = 1836$, box size $L = 512c/\omega_{pe}$, number of grid cells $n_g = 4096$, 1000 particles per cell per species, time step $\Delta t = 0.01/\omega_{pe}$, and maximum simulation time $t_{\max} = 655.36/\omega_{pe}$. Low-frequency fluctuations (right panels) are obtained from hybrid simulations with $L = 502.6v_A/\Omega_p$, $n_g = 4096$, and the same number of particles per cell, time step, and maximum running time. Although hybrid codes minimize electron dynamics and may lead to some minor differences contrasting with theory, both simulated spectra closely resemble the corresponding sets of high- and low-frequency fluctuations in Figure 2.

Suprathermal spectral components corresponding to quasi-parallel and quasi-perpendicular fluctuations in Figure 2 result from Equation (1), and are displayed in Figure 4 as $\text{Sign}[\langle \delta E^2 \rangle_{k,\omega}^{\text{st}}] \log |\langle \delta E^2 \rangle_{k,\omega}^{\text{st}}|$ (color levels). Positive values confirm, as shown by the color levels of red, a systematic stimulation of the spontaneous emissions of fast modes, e.g., Langmuir, fast magnetosonic, O- and X-modes, and the low-wavenumber branches of Alfvén and Bernstein waves, with a high enough phase speed. Indeed, these modes with $v_{\text{phase}} \equiv \omega/k$ are sufficiently high, e.g., $v_{\text{phase}} \geq v_{Ta}$ can be resonantly amplified by the suprathermal (energetic) particles with $v \geq v_{Ta}$, satisfying Landau resonance ($v_{\text{phase}} \simeq v$) or cyclotron resonance ($\omega \simeq |\Omega_a| - kv$). In Figure 4 we overplot these conditions as functions of thermal velocities, Landau resonance $\omega/k = v_{Ta}$ (dashed lines), and cyclotron resonance $\omega \simeq |\Omega_a| - kv_{Ta}$ (solid lines) for both the high-frequency emissions triggered by the electrons ($a=e$), and the low-frequency fluctuations mainly driven by the protons ($a=p$). As expected, suprathermal emissions are peaked by the fast modes above these conditions and for sufficiently low wavenumbers. Thermal emissions of a low phase speed involve (resonantly) the less-energetic particles from the core ($\omega/k \sim v < v_{\text{th}}$),

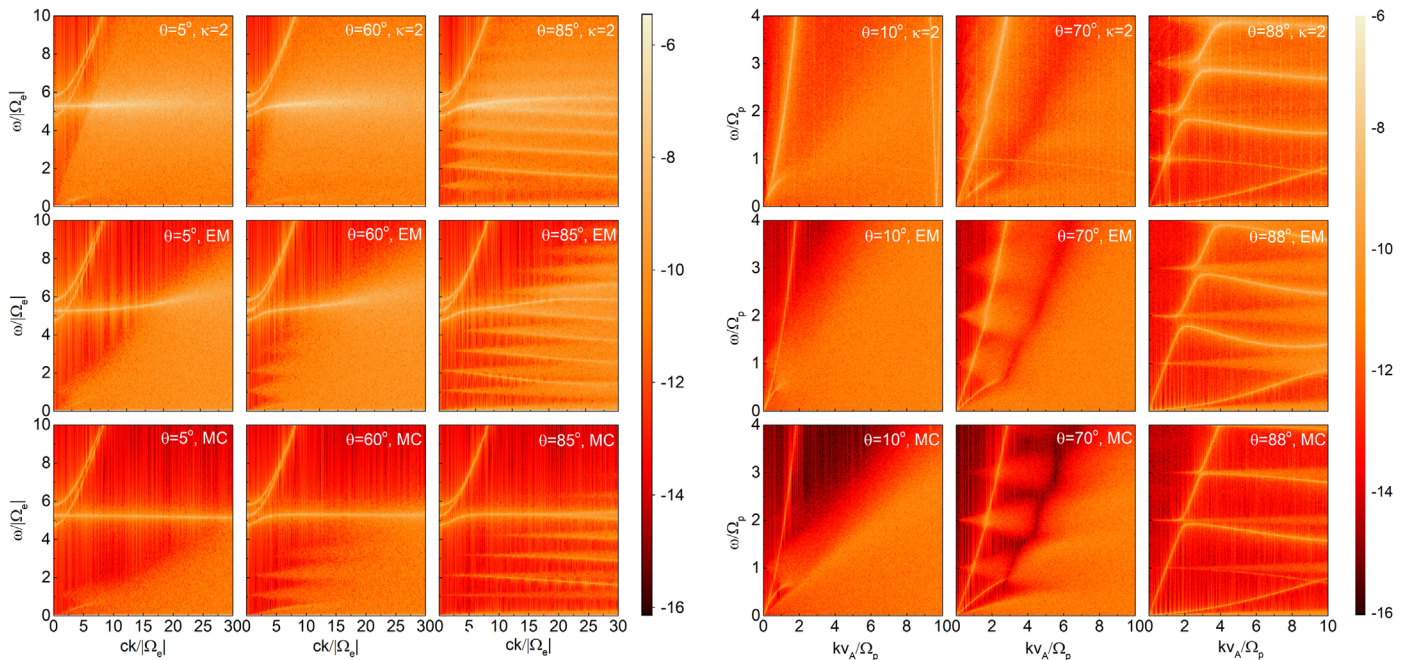


Figure 3. Fluctuations from simulations: high frequency (left) and low frequency (right).

which is slightly less populated than MC and may thus explain the negative (and not zero) values in blue areas. Enhanced thermal fluctuations are indeed obtained in the range of slow modes, see MC in Figures 2 and 3. Instead, spontaneous emissions in the range of fast modes are heavily dominated by the suprathermal fluctuations. Suprathermals should therefore facilitate detection of these spontaneous emissions, which include the high-frequency Langmuir fluctuations currently adopted in QTN spectroscopy. Originally developed for unmagnetized plasmas, these techniques have also been adjusted to weakly magnetized plasmas with κ -distributed electrons to determine their properties at large heliocentric distances in the solar wind, and, implicitly, some of the ion parameters (Zouganelis 2008). The error margins are below 10% for the electrons, but exceed 15% for protons, presumably, due to their very low QTN in the range of high-frequency (Langmuir) fluctuations. In the present computations of high-frequency emissions, e.g., in Figure 1 (left) we have also neglected the proton contribution, which is however captured by the simulations in Figure 2 (left) as a very low (background) noise without a sensitive influence on the peaks. Present results suggest that proton parameters may be extracted more accurately from the low-frequency fluctuations, e.g., in Figures 2–4, which here are computed assuming both the electrons and protons κ -distributed, with the same $\kappa = 2$. Heavier species may be more thermalized than electrons, and a Maxwellian calibration of their emissions can be acceptable (Zouganelis 2008), but even a faint suprathermal component, if present, it may be identified in the suprathermal emissions of low-frequency modes. Notice also that suprathermal fluctuations quantified in Equation (1) are a measure of the kinetic energy of suprathermal populations in quasi-stationary states, when emissions are constant in time being (partially) counter-balanced by the absorptions. In the presence of instabilities, e.g., driven by the temperature anisotropy of plasma particles, fluctuations are markedly enhanced by the induced emissions that increase the level of fluctuating field near the instability

thresholds, even in the absence of suprathermal populations (Bale et al. 2009; Navarro et al. 2014b). However, in the presence of suprathermals with an additional free energy these instabilities are stimulated (Lazar et al. 2015), leading to enhanced fluctuations (Viñas et al. 2015). Comparing to these theories that pertain to parallel propagation, our present results suggest how to estimate the full spectrum of induced fluctuations, which grow much faster in the oblique directions. In particular, suprathermal component of stimulated fluctuations can be estimated with a similar approach based on Equation (1), thus creating premises for an advanced diagnosis of the unstable states of anisotropic plasmas.

4. Conclusions

To conclude, suprathermal populations present in space plasmas have a significant contribution to the spontaneous emissions of electric and magnetic fields, and selectively enhance the fluctuations of fast modes, reflected by their peaking intensities in Figure 4. The electrons contribute mainly to high-frequency emissions, while suprathermal protons generate low-frequency fluctuations. In order to outline the magnitude of these emissions we invoke significant populations of suprathermal electrons and protons, as quantified by the low values of power-index, e.g., $\kappa_e = \kappa_p = 2$. Low values of κ reported by the observations are more typical of the solar wind electrons (Pierrard & Lazar 2010), but energized protons should also be present in the hotter corona, or even in the solar wind and terrestrial magnetosphere during the energetic coronal ejections (Haaland et al. 2010). Reducing the suprathermal component of protons (by increasing κ_p) does not affect the high-frequency emissions, but diminishes the lower frequency power spectra (a detailed study will be presented elsewhere).

The existing techniques of QTN spectroscopy involving the electrostatic fluctuations (Chateau & Meyer-Vernet 1991; Zouganelis 2008; Le Chat et al. 2009; Martinovic et al. 2018) may need a recalibration to take into account these selective patterns of suprathermal emissions, as estimated here

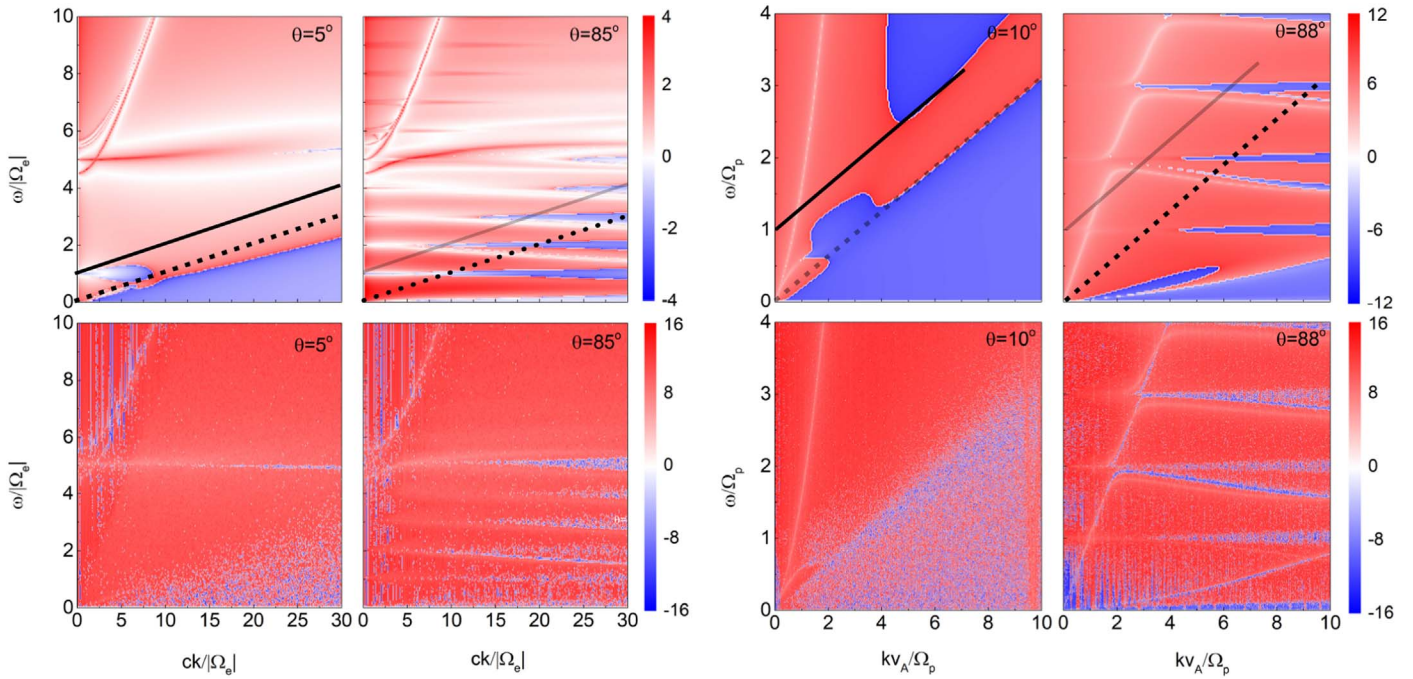


Figure 4. Suprathermal emissions from theory (top) and simulations (bottom): high frequency (left) and low frequency (right).

for a magnetized plasma, and compare with the fluctuations measured in situ. We are aware that the application of our theory to actual observation is not straightforward, in particular, when the total measured electric field power corresponds to the summation of fluctuations emitted in all directions. First we could point out that actual spacecraft measurement is on frequency, not both frequency and wave-vector, so in principle one should integrate over all wave-vectors k . However, as Meyer-Vernet et al. (2017) discussed, the integration over wave-vector must be done with the antenna geometrical factor multiplied, which effectively reduces the wave-vector integration into a 1D k -integration over antenna axis. This is equivalent to performing integration over modulus of k , while leaving the propagation angle as a free parameter. How to choose the propagation must depend on the local solar wind magnetic field direction and the spacecraft spin axis. The application of our theory to actual observation probably requires intimate knowledge of the spacecraft itself. The electrostatic emissions may present some facilities in this case, as the orientation of linear antenna used to measure them with respect to the spin axis or the magnetic field direction is known.

The electromagnetic emissions are less damped and are therefore expected to be more susceptible to remote detection with sensitive radio receivers, and ensure complementary means for an accurate diagnosis of particle distributions and their macroscopic properties. Details of the power spectra, including the inherent suprathermal component, should enable to refine capabilities of alternative diagnosis of high interest for the new heliospheric missions, which aim to explore regions in the outer corona where direct measurements of plasma particle flows are technically impossible. We may thus hope that peaking patterns of suprathermal emissions inferred from the spectral measurements of the newly launched PSP can confirm the coronal origin of the suprathermal populations that are observed in the solar wind.

The authors acknowledge support by the Deutsche Forschungsgemeinschaft (Schl 201/35-1, GSC 98/3, Schl 201/31-1), FWO-Vlaanderen (G0A2316N), National Research Foundation of Korea (2016R1A5A1013277-UNIST, and BK21 plus program to Kyung Hee University), NSF grant AGS1550566, and Science Award from GFT Charity Inc. to the University of Maryland. Useful discussions are acknowledged within the team Kappa Distributions at the first ISSI meeting in Bern.

ORCID iDs

M. Lazar  <https://orcid.org/0000-0002-8508-5466>
P. H. Yoon  <https://orcid.org/0000-0001-8134-3790>
R. Schlickeiser  <https://orcid.org/0000-0003-3171-5079>
S. Poedts  <https://orcid.org/0000-0002-1743-0651>

References

- Adrian, M. L., Viñas, A. F., Moya, P. S., & Wendel, D. E. 2016, *ApJ*, **833**, 49
Bale, S. D., Goetz, K., Harvey, P. R., et al. 2016, *SSR*, **204**, 49
Bale, S. D., Kasper, J. C., Howes, G. G., et al. 2009, *PhRvL*, **103**, 211101
Chateau, Y. F., & Meyer-Vernet, N. 1991, *JGR*, **96**, 5825
Goldstein, M. L., Wicks, R. T., Perri, S., & Sahraoui, F. 2015, *RSPTA*, **373**, 20140147
Haaland, S., Kronberg, E. A., Daly, P. W., et al. 2010, *AnGeo*, **28**, 1483
Hoang, S., Meyer-Vernet, N., Moncuquet, M., Lecacheux, A., & Pedersen, B. M. 1993, *P&SS*, **41**, 1011
Issautier, K., Meyer-Vernet, N., Moncuquet, M., & Hoang, S. 1998, *JGR*, **103**, 1969
Kim, S., Lazar, M., Schlickeiser, R., López, R. A., & Yoon, P. H. 2018, *PPCF*, **60**, 075010
Kim, S., Schlickeiser, R., Yoon, P. H., López, R. A., & Lazar, M. 2017, *PPCF*, **59**, 125003
Lazar, M., Poedts, S., & Fichtner, H. 2015, *A&A*, **582**, A124
Le Chat, G., Issautier, K., Meyer-Fernet, N., et al. 2009, *PhPI*, **16**, 102903
López, R. A., Viñas, A. F., Araneda, J. A., & Yoon, P. H. 2017, *ApJ*, **845**, 60
López, R. A., & Yoon, P. H. 2017, *PPCF*, **59**, 115003
Maksimovic, M., Hoang, S., Meyer-Vernet, N., et al. 1995, *JGR*, **100**, 19881
Martinovic, M. M., Zaslavsky, A., Maksimovic, M., et al. 2018, *JGRA*, **121**, 129

- Meyer-Vernet, N. 1979, *JGR*, **84**, 1
- Meyer-Vernet, N., & Issautier, K. 1998, *JGR*, **103**, 29705
- Meyer-Vernet, N., Issautier, K., & Moncuquet, M. 2017, *JGRA*, **122**, 7925
- Meyer-Vernet, N., & Perche, C. 1989, *JGR*, **94**, 2405
- Moncuquet, M., Lecacheux, A., Meyer-Vernet, N., Cecconi, B., & Kurth, W. S. 2005, *GeoRL*, **32**, L20S02
- Müller, D., Marsden, R. G., Cyr, O. C., St., Gilbert, H. R. & The Solar Orbiter Team 2013, *SoPh*, **285**, 25
- Navarro, R. E., Araneda, J. A., Muñoz, V., et al. 2014a, *PhPI*, **21**, 092902
- Navarro, R. E., Moya, P. S., Muñoz, V., et al. 2014b, *PhRvL*, **112**, 245001
- Navarro, R. E., Muñoz, V., Araneda, J., et al. 2015, *JGR Space Physics*, **120**, 2382
- Pierrard, V., & Lazar, M. 2010, *SoPh*, **267**, 153
- Schlickeiser, R., & Yoon, P. H. 2012, *PhPI*, **19**, 022105
- Vasyliunas, V. M. 1968, *JGR*, **73**, 2839
- Viñas, A. F., Mace, R. L., & Benson, R. F. 2005, *JGR*, **110**, A06202
- Viñas, A. F., Moya, P. S., Navarro, R., & Araneda, J. A. 2014, *PhPI*, **21**, 012902
- Viñas, A. F., Moya, P. S., Navarro, R. E., et al. 2015, *JGRA*, **120**, 3307
- Yoon, P. H., Hwang, J., López, R. A., Kim, S., & Lee, J. 2018, *JGRA*, **123**, 5356
- Yoon, P. H., & López, R. A. 2017, *PhPI*, **24**, 022117 erratum, Yoon, P. H., & López, R. A. 2017, *PhPI*, **24**, 049902
- Zouganelis, I. 2008, *JGR*, **113**, A08111